Fault location and source process of the Boumerdes, Algeria, earthquake inferred from geodetic and strong motion data

Fethi Semmane,[1] Michel Campillo, and Fabrice Cotton

Laboratoire de Géophysique Interne et Tectonophysique, Observatoire de Grenoble, Université Joseph Fourier and CNRS, Grenoble, France

Received 16 August 2004; revised 12 November 2004; accepted 7 December 2004; published 8 January 2005.

[1] The Boumerdes earthquake occurred on a fault whose precise location, offshore the Algerian coast, was unknown. Geodetic data are used to determine the absolute position of the fault. The fault might emerge at about 15 km offshore. Accelerograms are used to infer the space-time history of the rupture using a two-step inversion in the spectral domain. The observed strong motion records agree with the synthetics for the fault location inferred from geodetic data. The fault plane ruptured for about 18 seconds. The slip distribution on the fault indicates one asperity northwest of the hypocenter with maximum slip amplitude about 3 m. This asperity is probably responsible for most of the damage. Another asperity with slightly smaller slip amplitude is located southeast of the hypocenter. The rupture stops its westward propagation close to the Thenia fault, a structure almost perpendicular to the main fault.
Citation: Semmane, F., M. Campillo, and F. Cotton (2005), Fault location and source process of the Boumerdes, Algeria, earthquake inferred from geodetic and strong motion data, *Geophys. Res. Lett.*, *32*, L01305, doi:10.1029/2004GL021268.

1. Introduction

[2] The 21 May 2003 Boumerdes earthquake (sometimes called Zemmouri earthquake) of moment magnitude Mw = 6.9 occurred in one of the most seismically active regions in the western Mediterranean Sea. It was relocated by *Bounif et al.* [2004] at 36.83N–3.65E on the coast of the Boumerdes prefecture, immediately east of Algiers. USGS, Harvard, EMSC and the Algerian seismological center CRAAG (Research Center in Astronomy, Astrophysics and Geophysics) gave locations several kilometers offshore. The focal mechanism indicates a thrust-faulting event. This earthquake induced a tsunami recorded about one hour later at the Balearic Islands [*Ayadi et al.*, 2003; *Hebert and Alasset*, 2003]. Neither the precise geometry nor the location of the fault which generated the Boumerdes earthquake was known before the event because no fault mapping has ever been done offshore of Algeria. The first results of the 2003 summer MARADJA cruise (Algerian active margin investigation 3 months after the event) show the surface traces of three fault segments, which could be a part of the fault activated during the Boumerdes earthquake [*Déverchère et al.*, 2003]. These segments are located at about 15–20 km offshore. *Yelles et al.* [2004] using the GPS data showed that the surface projection of the top of the fault is situated at 6 km offshore, and the bottom of the fault at 4 km inland. *Meghraoui et al.* [2004] using the uplifts and the leveling data suggested that the fault might emerge between 5–10 km offshore.

[3] Since the distribution of static deformations is highly sensitive to fault position, our first goal in this study is to find the best absolute position of the fault using all available geodetic data (GPS, uplifts and leveling). The second goal is to take advantage of near source strong motion records to derive a space-time history of rupture on this fault plane using a nonlinear two-step inversion: in the first step we compute the static solution by inverting the geodetic deformation field to constrain the slip distribution on the fault. In the second step, we infer the slip history on the fault plane by inverting the strong-motions using as starting model the static solution. This procedure is detailed by *Hernandez et al.* [1999].

2. Geodetic Data

[4] The fault, which generated the Boumerdes earthquake, was not mapped before the event. Therefore, neither seismological nor geodetic network were installed specifically to monitor this fault. The GPS data consist of horizontal displacements recorded at 9 stations installed by CRAAG two months before the event for monitoring the Thenia fault [*Boudiaf*, 1996]. Consequently, only the SW part of the epicentral area is covered by GPS stations (Figure 1). Some stations were installed on the roof of low buildings, others directly on the ground. The remarkable coherence of the displacements (one sole direction, Figure 2) shows that there is little doubt on the fact that the direction of the static motions is not affected by the building deformation.

[5] The GPS data can be divided in three categories (see Figure 1 and Figure 2). Relatively small displacements are recorded at two adjacent stations located west of the fault in the Ain-Taya peninsula (ATY and MAR). A group of records (six) in a small area in the western termination of the fault shows one sole direction of the displacement, while at station ZEM a significant displacement of about 10 cm is in an opposite direction to all other records.

[6] During this earthquake, a spectacular uplift of the coast has been observed in the epicentral area (thick coastline in Figure 1). A maximum value of about 75 cm was measured at Boumerdes. The uplifts values have been measured and corrected from the tide effect (which has an amplitude of about 15 cm) by *Meghraoui et al.* [2004]. The large gap in the measurements along the coast (about 20 km long) is due to the presence of sand beaches. These observations are included in our analysis as well as

[1] Also at Centre de Recherche en Astronomie, Astrophysique et Géophysique, Observatoire d'Alger, Bouzaréah Alger, Algeria.

0094-8276/05/2004GL021268$05.00

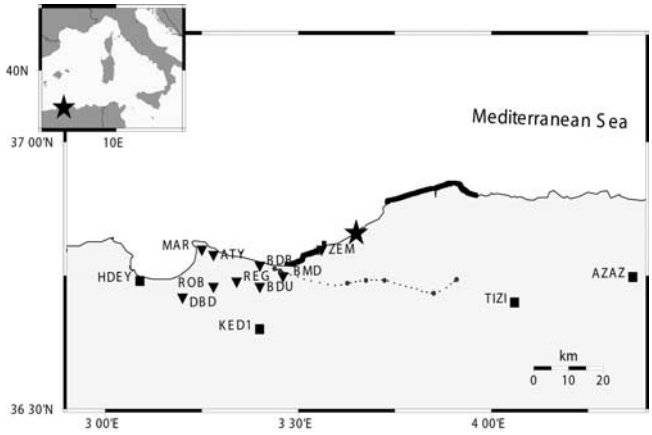

Figure 1. Star is the epicenter, squares are strong-motion stations, triangles are GPS stations, dashed line is the leveling-line, and the thick line is the measured uplift coastline. BMD: Boumerdes. ZEM: Zemmouri.

7 leveling measurements performed along a railroad south of the epicentral area (dashed line on Figure 1).

3. Strong Motion Data and Velocity Structure Model

[7] The Boumerdes earthquake has been recorded by stations of the accelerometric network (335 stations) managed and maintained by CGS, the Algerian earthquake engineering research center [*Laouami et al.*, 2003]. We choose four strong motion stations (Figure 1) among those which recorded the main shock on the following criteria: fault proximity, free field, azimuthal distribution, absence of visible 3D wave-propagation-effect (some stations installed in the Mitidja basin show indications of site effects such as late arrivals which could be explained by surface waves generated at the edges of the sedimentary basin). Among these four stations only one is digital (Keddara, Kinemetrics ETNA), the others are analogic (SMA-1). There is no absolute time available on the analogic stations. The data set consists of 12 strong-motion components. In the initial model we considered a constant initial slip of 30 cm for each subfault (which leads to a starting moment magnitude equal to 6.9), a rise time equal to 1.4 s and a constant rupture velocity equal to 2800 m/s. A smoothed ramp function is used as source time function.

[8] The flat layered-velocity model considered here is derived from the one used by CRAAG for the location of local events (H. Beldjoudi, personal communication, 2003). Our model consists of 3 layers of thickness equal to 2, 10, 22 km overlying a half space. The P-wave velocities are 4.5, 5.0, 6.5 and 8.0 km/s. The shear velocities are 2.10, 2.89, 3.71 and 4.62 km/s while the densities are 2.50, 2.67, 2.70 and 2.78 respectively.

4. Boumerdes Earthquake Source Process

[9] We considered the fault plane orientation given by teleseismic inversion results (USGS CMT) as a fixed parameter. The fault plane is dipping 47° to the SE and has a strike of 54°. The rake is 88°. This fault orientation is close to the one given by other teleseismic inversions, e.g., Harvard CMT, and Yagi's model (available at //iisee.kenken.go.jp/staff/yagi/eq/algeria20030521/algeria2003521.html). The fault surface on which we consider that slip may occur is 64 km long and 32 km wide, extending between 1 km and 23 km in depth.

4.1. Static Displacement and Fault Location

[10] To model static deformation we used a layered crustal model rather than a half space to avoid overestimating the horizontal displacement as it was shown by *Savage* [1998] and *Cattin et al.* [1999].

[11] The geodetic data, in particular horizontal displacement vectors, are highly sensitive to fault position compared to other type of data, e.g. teleseismic [*Hernandez et al.*, 1999]. We performed several inversions assuming different positions of the fault plane but keeping fixed the dip, strike and rake. Coastal uplift and leveling measurements are given less weight than GPS data for the inversion. All GPS displacements are equally weighted. In Figure 2 we show how geodetic data are fitted when considering three particular fault positions at distances of about 7, 15 and 21 km from the top of the fault to the shoreline (the epicenter is fixed for the 3 locations then only the focus depth is changing).

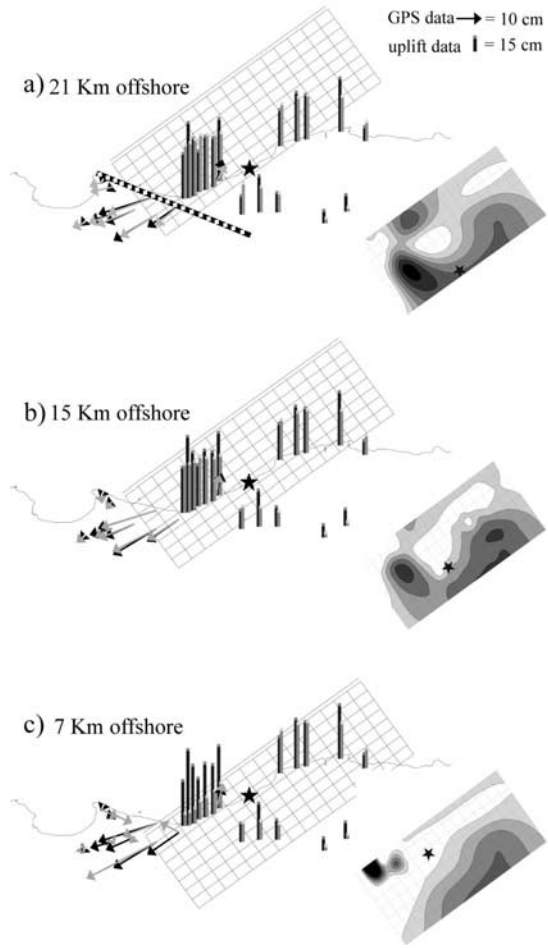

Figure 2. Three positions of the fault are showed: fault emergence at 7 km, 15 km or 21 km far from the coast. The corresponding slip distributions are shown on the right. Arrows are horizontal displacement vectors; vertical columns are uplifts (on the coast) and leveling south of the epicentre (star). Data are in black and synthetics are in gray. Thick dashed line in a) is the vertical Thenia fault.

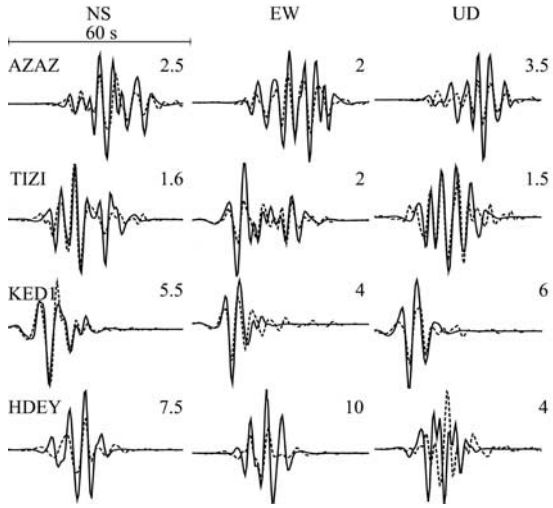

Figure 3. Observed (solid line) and synthetics (dashed line) waveforms comparison. Numbers at each trace show the maximum displacement value in cm.

These positions are chosen with respect to the hypothesis emitted after post-seismic inland field investigations and offshore studies. *Ayadi et al.* [2003] and *Meghraoui et al.* [2004] suggest that the fault would emerge close to the coast between distances 5 and 10 km. The first report of the Algerian active margin investigation suggests that the fault would emerge farther than 5–10 km [*Déverchère et al.*, 2003]. We performed the inversion for the 3 fault locations and found that the fault at 15 km offshore provides the best fit to the whole data set. Figure 2 indicates that when the fault plane is put closer to the coast (7 km) we obtain the worst fit to the geodetic data among the 3 cases considered, particularly for the GPS data. The slip distributions on the fault plane obtained for the 3 fault locations are shown in Figures 2a, 2b and 2c. Two main regions of large slip are obtained: one in the west, centered at about 14 km along dip (10 km depth), the second, deeper to the east and in between a zone of weak slip in the hypocentral region.

4.2. Strong-Motion Inversion

[12] According to the results of the inversion done for static displacement only, we consider in the following a fault 15 km offshore as discussed in the previous section. Following *Hernandez et al.* [1999], we use a two-step inversion in which the slip distribution derived from geodetic data (Figure 2b) is used as the a priori model for strong motion inversion. The original acceleration waveforms were band pass filtered in the frequency range [0.1–0.5] Hz using a two-pole Butterworth filter applied forward and backward and finally doubly integrated to obtain particle displacement. All strong motion components are equally weighted. We invert for the displacement in the spectral domain [*Cotton and Campillo*, 1995]. Figure 3 shows a comparison between observed displacement (solid line) and calculated displacement (dashed line). All records are well fitted (variance reduction = 58%) although the waveforms are complex, especially at stations TIZI and AZAZ. Such a good agreement for stations close to the fault plane confirms the fault location that we deduced independently from the static displacements. The slip distribution inferred from the two-step inversion is shown in Figure 4a. The patch southeast of hypocenter is more expressed (compared to Figure 2b) otherwise the global shape found with geodetic data is confirmed with a slight increase of the maximum slip amplitude (2.9 m). In the high slip regions the rake is vertical with very slight variation. In Figure 4b is shown the rupture front evolution. The fault plane ruptured for about 18 s.

[13] Although the propagation of the rupture is bi-lateral, the directivity effect can be observed on land where it affects the intensity of strong ground motion and produces large amplitude transverse motion at Keddara (KED) and Hussein-Dey (HDEY).

[14] *Kherroubi et al.* [2004] presented a preliminary location of aftershocks recorded following the Boumerdes earthquake. Their epicenters lie on the surface projection of our preferred fault plane. The depth of the aftershocks unfortunately could not inform us about the absolute location of the fault since the aftershocks could (in the case of a thrust faulting) occur either in the hanging wall, e.g. the 1999 Chichi earthquake where most of the aftershocks relocated by *Chang et al.* [2000] occurred in the hanging wall or, e.g., the 1980 El-Asnam earthquake where the aftershocks were located in the footwall and/or in the hanging wall depending on which part of the fault is considered [*Yielding et al.*, 1989].

5. Discussion and Conclusion

[15] We use near field geodetic data to constrain the absolute position of the fault whose orientation is given by previous teleseismic data analysis. It leads to a model in which the surface trace of the fault is at about 15 km in front of GPS station ZEM. Among the geodetic data, the GPS horizontal displacement vectors are the most sensitive to the

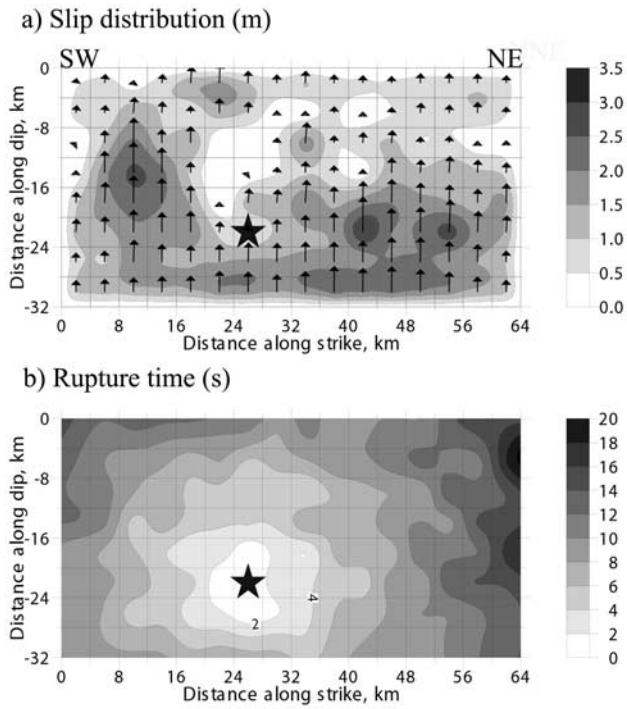

Figure 4. (a) Slip model distribution inferred from a 2-step inversion (b) Rupture front evolution.

fault location as shown by Figure 2. The fault location, fault geometry and slip distribution are well constrained on the western part of the fault because all GPS stations are located in the west. In the eastern part, however, the only data available are uplifts and leveling (vertical movements). Yet, as shown in Figure 2 the vertical movements may be explained by different fault positions relative to the coast, provided that we put the required slip amplitude. The position of our fault plane, also, agrees with the first results of the investigations of the Algerian margin by *Déverchère et al.* [2003]. The fault geometry (fault orientation and absolute location) allows fitting the strong-motion records at the 4 near source stations. The space-time history of rupture has therefore been derived. The fault plane ruptured for about 18 seconds and slip on the fault consists in two large slip zones. The largest is located to the west of the hypocenter with slip amplitude about 3 m. The surface projection of this lies between 2 km inland and 9 km offshore. Another asperity with slightly smaller slip amplitude is located southeast of the hypocenter. Performing geodetic, strong-motions or a 2-step inversion with different starting models (uniform slip or a model derived from GPS inversion), the result always consists in two large slip areas located on both side of the hypocenter. The model, which gives the best fit to the data, has a seismic moment of about 5.9×10^{19} N m (Mw = 7.1). Other inversions (Yagi's model, available at //iisee.kenken.go.jp/staff/yagi/eq/algeria20030521/algeria2003521.html) [*Delouis et al.*, 2004] also show two large slip areas on both side of the hypocenter. The eastern asperity positions along dip differ among the different studies. Our model is close to Yagi's one while *Delouis et al.* [2004], performing a joint geodetic-teleseismic inversion, suggested a shallower asperity east of the hypocenter. Another main difference is the moment magnitude that is found relatively higher in our study. In our opinion, these differences are due to the lack of data in the eastern part to constrain the fault location and slip distribution. Using the static solution as starting model we could easily fit the strong-motions. We performed tests showing that the reciprocal is not true: the model obtained inverting the strong-motions alone does not explain geodetic observations. Indeed, using the four strong-motion stations alone, the matrix resolution indicates that less than 30% of the model parameters are actually resolved. The western rupture termination of the Boumerdes earthquake could be related to the presence of the almost perpendicular Thenia fault [*Boudiaf*, 1996] as shown in Figure 2a. Several examples of rupture propagation controlled by a complex fault system are discussed by I. Manighetti et al. (Evidence for self-similar, triangular slip distributions on earthquakes: Implications for earthquake and fault mechanics, submitted to *Journal of Geophysical Research*, 2005).

[16] **Acknowledgments.** We thank Nasser Laouami (CGS) for providing us with strong motion data, Mustapha Meghraoui and Catherine Dorbath (IPGS) for providing us with the uplifts data and epicenter relocation, Karim Yelles (CRAAG) for providing GPS data and for discussions and support. We acknowledge helpful discussions on the fault position with Jacques Déverchère. Thanks to Christophe Voisin and Marc Kham to their comments to improve the paper. Martin Mai and two anonymous reviewers gave valuable suggestions to improve the paper. We benefited from the support of the program ACI "Aléas et changements globaux".

References

Ayadi, A., et al. (2003), Strong Algerian earthquake strikes near capital city, *Eos Trans. AGU*, *84*(50), 561, 568.

Boudiaf, A. (1996), Etude sismotectonique de la région d'Alger et de la Kabylie, Ph.D. dissertation, Univ. of Montpellier, Montpellier, France.

Bounif, A., et al. (2004), The 21 May 2003 Zemmouri (Algeria) earthquake Mw 6.8: Relocation and aftershock sequence analysis, *Geophys. Res. Lett.*, *31*, L19606, doi:10.1029/2004GL020586.

Cattin, R., P. Briole, H. Lyon-Caen, P. Bernard, and P. Pinettes (1999), Effects of superficial layers on coseismic displacements for a dip-slip fault and geophysical implications, *Geophys. J. Int.*, *137*, 149–158.

Chang, C. H., Y. M. Wu, T. C. Shin, and C. Y. Wang (2000), Relocation of the 1999 Chi-Chi Earthquake in Taiwan, *J. Terr. Atmos. Ocean. Sci.*, *11*(3), 581–590.

Cotton, F., and M. Campillo (1995), Inversion of strong ground motion in the frequency domain. Application to the 1992 Landers, California earthquake, *J. Geophys. Res.*, *100*, 3961–3975.

Delouis, B., M. Vallée, M. Meghraoui, E. Calais, S. Maouche, K. Lammali, A. Mahsas, P. Briole, F. Benhamouda, and K. Yelles (2004), Slip distribution of the 2003 Boumerdes-Zemmouri earthquake, Algeria, from teleseismic, GPS, and coastal uplift data, *Geophys. Res. Lett.*, *31*, L18607, doi:10.1029/2004GL020687.

Déverchère, J., K. Yelles, and E. Calais (2003), Active deformation along the Algerian Margin (MARADJA cruise): Framework of the May 21, 2003, Mw-6.8 Boumerdes earthquake, *Eos Trans. AGU*, *84*(46), Fall Meet. Suppl., Abstract S42E-0216.

Hebert, H., and P.-J. Alasset (2003), The tsunami triggered by the 21 May 2003 Algiers earthquake, *CSEM Newsl.*, *20*, 10–12.

Hernandez, B., F. Cotton, and M. Campillo (1999), Contribution of radar interferometry to a two-step inversion of the kinematics process of the 1992 Landers earthquake, *J. Geophys. Res.*, *104*, 13,083–13,100.

Kherroubi, A., H. Beldjoudi, A. Yelles, S. Maouche, F. Oussadou, M. Meghraoui, and A. Ayadi (2004), The Boumerdes-Zemmouri (Algeria) Earthquake (Mw = 6.8) on May 21st 2003: First results of the aftershocks sequence, paper presented at first meeting, Eur. Geophys. Union, Nice, France, 25–30 April.

Laouami, N., A. Slimani, Y. Bouhadad, A. Nour, and S. Larbes (2003), Analysis of Strong Ground Motions Recorded during the 21st May, 2003 Boumerdes, Algeria, Earthquake, *CSEM Newsl.*, *20*, 5–7.

Meghraoui, M., S. Maouche, B. Chemaa, Z. Cakir, A. Aoudia, A. Harbi, P.-J. Alasset, A. Ayadi, Y. Bouhadad, and F. Benhamouda (2004), Coastal uplift and thrust faulting associated with the M_w = 6.8 Zemmouri (Algeria) earthquake of 21 May, 2003, *Geophys. Res. Lett.*, *31*, L19605, doi:10.1029/2004GL020466.

Savage, J. C. (1998), Displacement field for an edge dislocation in a layered half-space, *J. Geophys. Res.*, *103*, 2439–2446.

Yelles, K., K. Lammali, A. Mahsas, E. Calais, and P. Briole (2004), Coseismic deformation of the May 21st, 003, M_w = 6.8 Boumerdes earthquake, Algeria, from GPS measurements, *Geophys. Res. Lett.*, *31*, L13610, doi:10.1029/2004GL019884.

Yielding, G., M. Ouyed, G. C. P. King, and D. Hatzfeld (1989), Active tectonics of the Algerian Atlas Mountains—Evidence from aftershocks of the 1980 El-Asnam earthquake, *Geophys. J. Int.*, *99*(3), 761–788.

M. Campillo, F. Cotton, and F. Semmane, Laboratoire de Géophysique Interne et Tectonophysique, Observatoire de Grenoble, Université Joseph Fourier and CNRS, Grenoble F-38400, France. (fethi.semmane@obs.ujf-grenoble.fr)